



Fabric/multi-walled carbon nanotube sensor for portable on-site copper detection in water

Yang Lu¹ · Guoqiang Yu² · Xin Wei^{3,4} · Chuanxing Zhan⁴ · Ju-Won Jeon⁵ · Xifang Wang⁶ · Clayton Jeffryes³ · Zhanhu Guo⁷ · Suying Wei^{3,4} · Evan K. Wujcik^{1,3,8,9} 

Received: 10 January 2019 / Revised: 12 September 2019 / Accepted: 14 October 2019 / Published online: 31 October 2019
© Springer Nature Switzerland AG 2019

Abstract

Excessive copper (as Cu(II)) in drinking water—in place through mining, farming, manufacturing operations, and municipal or industrial wastewater releases—can be a threat to human health and ecosystem wellbeing. Some sources of drinking water are remote; hence, the sensitive, selective, and portable detection of contaminated copper in drinking water sources is of great importance. Through this work, a portable fabric amperometric nanosensor has been devised via a simple dip-coating method, which is able to rapidly, sensitively, and selectively detect Cu(II) ions in a range of 0.65 to 39 ppm in real time. The prepared Cu(II) nanosensor, which operates under a low voltage, consists of three layers: electrospun nylon-6 nanofibers, multi-walled carbon nanotubes, and 2,2':5',2''-terthiophene molecules. Potential interfering metal ions, including Cd(II), Fe(II), Pb(II), Hg(II), and Ag(I) ions, have no significant influence on the response of the Cu(II) nanosensor. This fabric sensor—that is able to be placed in your pocket and carried about—is more portable than current technologies, while being able to detect Cu(II) on the same level necessary for potable water. We anticipate our nanosensor to be a starting point for more sophisticated and comprehensive heavy metal assay. Furthermore, this nanosensor will aid in on-site detection of Cu(II) in potential drinking water sources, lending itself well to third world and remote detection.

Keywords Portable Cu(II) sensor · Water monitoring · Carbon nanotubes · Electrospinning · Dip coating

1 Introduction

Potable water is vital to life, and that it is clean and safe to use is of utmost importance. However, millions of people still

suffer from the threats of unhealthy drinking water around the world, especially those living in third-world countries and remote locations. Copper is a naturally occurring metal—often classified as a heavy metal—found in rocks,

Yang Lu and Guoqiang Yu contributed equally to this work.

Electronic supplementary material The online version of this article (<https://doi.org/10.1007/s42114-019-00122-7>) contains supplementary material, which is available to authorized users.

✉ Evan K. Wujcik
Evan.Wujcik@ua.edu

¹ Materials Engineering And Nanosensor [MEAN] Laboratory, Department of Chemical and Biological Engineering, The University of Alabama, Tuscaloosa, AL 35487, USA

² Department of Chemistry, Virginia Tech, Blacksburg, VA 24061, USA

³ Dan F. Smith Department of Chemical Engineering, Lamar University, Beaumont, TX 77705, USA

⁴ Department of Chemistry and Biochemistry, Lamar University, Beaumont, TX 77705, USA

⁵ Department of Applied Chemistry, Kookmin University, Seoul 02701, Republic of Korea

⁶ Department of Materials Science and NanoEngineering, Rice University, Houston, TX 77005, USA

⁷ Integrated Composites Laboratory [ICL], Department of Chemical and Biomolecular Engineering, The University of Tennessee, Knoxville, TN 37996, USA

⁸ Department of Civil, Construction, and Environmental Engineering, The University of Alabama, Tuscaloosa, AL 35487, USA

⁹ Alabama Water Institute, The University of Alabama, Tuscaloosa, AL 35487, USA

soil, plant life, a number of organisms, and water [1]. Many of these organisms' diets—including humans—require copper in trace amounts; however, excessive or certain forms of copper have also been shown to cause gastrointestinal distress, liver disease, and kidney damage [2–4]. The highest level of copper in drinking water limited by the United States Environmental Protection Agency (U.S. EPA) is 1.3 mg/L (1.3 ppm) [5–7]. Therefore, it is crucial to be able to identify and detect the amount of copper in drinking water, if it is above the U.S. EPA limit.

Many aqueous elemental detection techniques have been developed previously. Conventional methods, including atomic absorption spectroscopy (AAS), atomic emission spectroscopy (AES), inductively coupled plasma mass spectrometry (ICP-MS), and inductively coupled plasma optical emission spectrometry (ICP-OES), have performances with excellent sensitivity, accuracy, and selectivity [8–12]. However, they require sophisticated instruments that are costly, time consuming, require expertise, and lack portability. Many new tools have occurred since the start of the twenty-first century, such as colorimetric sensors [13–16], “turn-on” or “turn-off” fluorescent probes [17–20], biosensors [21–23], square wave anodic stripping voltammetry [24–26], differential pulse voltammetry [27–29], and potentiometric measurements based on ion-selective electrodes [30–32]. They are not only more economic, portable, sensitive, and selective but also able to rapidly detect the concentrations of copper on site. Nevertheless, the processes to fabricate them are usually tedious, and particular chromogenic and fluorescent receptors, biological recognition elements, and electrode materials are often required to prepare.

Here, we propose a simple dip-coating procedure to fabricate a fabric amperometric sensor for the selective detection of Cu(II) ions in drinking water for the first time. The prepared Cu(II) sensor consists three layers. The bottom layer is nylon-6 nanofibers that are used as scaffolds to support the other two layers. The middle layer is composed of multi-walled carbon nanotubes (MWCNTs) which are utilized to yield a conductive sensing platform due to their superb electronic properties. The top layer is 2,2':5',2''-terthiophene molecules that have a high adsorption and selectivity towards Cu(II) ions [33]. Figure 1 illustrates the schematic diagram (macroscopic top view and nanoscale side view) of the Cu(II) sensor (2,2':5',2''-terthiophene/MWCNTs/nylon-6 nanocomposites) and the sensor response to the Cu(II) ions. When a voltage is applied to the Cu(II) sensor, a baseline current will be detected ascribed to the movement of charge carriers (electrons) in MWCNTs. As a tiny amount of water containing Cu(II) ions being added, the Cu(II) ions will be captured by the 2,2':5',2''-terthiophene molecules. Once that occurs, an impeded current can be observed, and the current impedance correlates with the concentration of Cu(II) ions in water. It is believed that the impedance results from the attraction of positively charged

Cu(II) ions to the negative electrons in MWCNTs [34]. In this work, the sensitivity and selectivity of the Cu(II) sensor are carefully studied.

2 Material and methods

Materials Nylon-6 pellets (polycaprolactam, 3 mm), acetic acid (ACS, $\geq 99.7\%$), formic acid (ACS, $\geq 98\%$), Triton X-100 (4-(1,1,3,3-tetramethylbutyl)phenyl-polyethylene glycol, 625 g/mol), and silver nitrate (AgNO_3 , ACS, $\geq 99\%$) were purchased from Sigma-Aldrich. Multi-walled carbon nanotubes (MWCNTs, outer diameter 10–20 nm, inside diameter 3–5 nm, length 10–30 μm , specific surface area 233 m^2/g , $> 95\%$) were supplied by Cheap Tubes, Inc. 2,2':5',2''-terthiophene ($\geq 98\%$) was obtained from Ark Pharm, Inc. Tetrahydrofuran (THF, certified) was purchased from Fisher Chemical. Copper chloride (CuCl_2 , 99%) and ferrous chloride (FeCl_2 , 97%) were purchased from Acros Organics. Cadmium chloride (CdCl_2 , 99.9%), lead nitrate ($\text{Pb}(\text{NO}_3)_2$, reagent), and mercury chloride (HgCl_2 , ACS) were purchased from Alfa Aesar.

Sensor preparation The nylon-6 nanofibers were fabricated via electrospinning. First, nylon-6 pellets were dissolved in 1:1 (w/w) acetic acid:formic acid solution at 20 wt%. Then, the nylon-6 solution was transferred into a 5-mL syringe and loaded into the syringe pump. The nylon-6 nanofiber mat was electrospun at a solution feed rate of 9.1 $\mu\text{L}/\text{min}$ for 4 h. A bias of 30 kV was applied between the syringe needle and rotating drum collector, between which was a distance of 8 cm. After that, the electrospun nylon-6 nanofiber mat was dried under vacuum at room temperature for 24 h.

A dip-coating procedure was employed to load MWCNTs and 2,2':5',2''-terthiophene molecules onto the nylon-6 nanofibers [34, 35]. The fabricated nylon-6 nanofiber mat was cut into rectangular pieces with sizes of 1 \times 2 cm and dipped into a bath in which MWCNTs were dispersed in a 0.3 wt% Triton X-100 aqueous solution. Triton X-100 was used as a surfactant to stabilize the MWCNTs in water. The concentration of MWCNTs aqueous solution was optimized at 0.25 g/L for the uniform dispersion on the surface of nylon-6, according to our previous work [36]. After 30 s, the nylon-6 nanofiber pieces were removed and placed in a water bath for 1 min to remove the loosely bound MWCNTs. The MWCNTs/nylon-6 nanocomposites were dried under ambient conditions, and then immersed in a 2.5 g/L 2,2':5',2''-terthiophene solution using THF as the solvent for 24 h to ensure the fully load of molecules. The Cu(II) sensors, MWCNTs/nylon-6 nanocomposites loaded with 2,2':5',2''-terthiophene, were prepared after they were dried under ambient conditions.

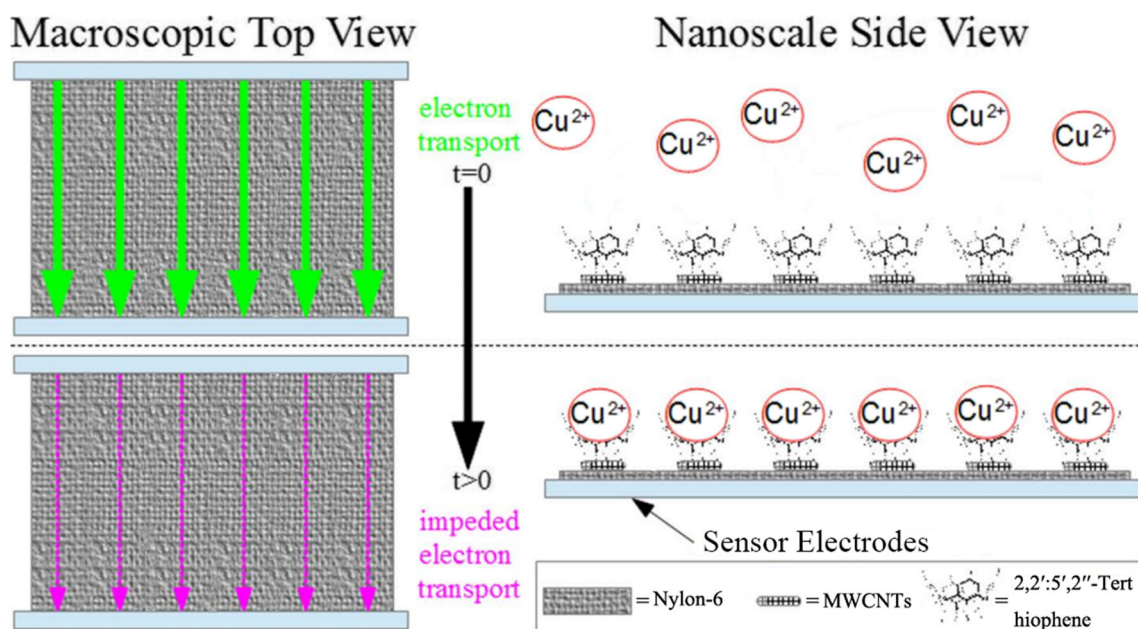


Fig. 1 Mechanism of detecting Cu(II) ions by 2,2':5',2''-terthiophene/MWCNTs/nylon-6 nanocomposites

Sensor evaluation All the electrochemical experiments were carried out utilizing the Solartron Analytical CellTest System which consisted of a 1470E multi-channel potentiostat unit and multiple 1455A series frequency response analyzers. The Cu(II) sensor was fixed on a glass slide with two nickel-plated steel alligator clips (each at one short side of the 1×2 cm sensor) connected to channel cables of the 1470E unit. To measure the resistivity, 30 μL of deionized water was dropped onto the Cu(II) sensor, and then a voltage ranging from -3 to 3 V in 2 min was applied to it. The changes in current with voltage were collected.

To characterize the responses of Cu(II) sensors to Cu(II) ions, CuCl_2 aqueous solutions in which the concentrations of Cu(II) ions were 0, 0.13, 0.65, 1.3, 6.5, 13, 39, and 65 ppm, respectively, were prepared. A constant voltage of 1 V was applied to the Cu(II) sensors, and 30 μL of those prepared CuCl_2 aqueous solutions were dropped after 30 s. The changes in currents within 5 min were recorded.

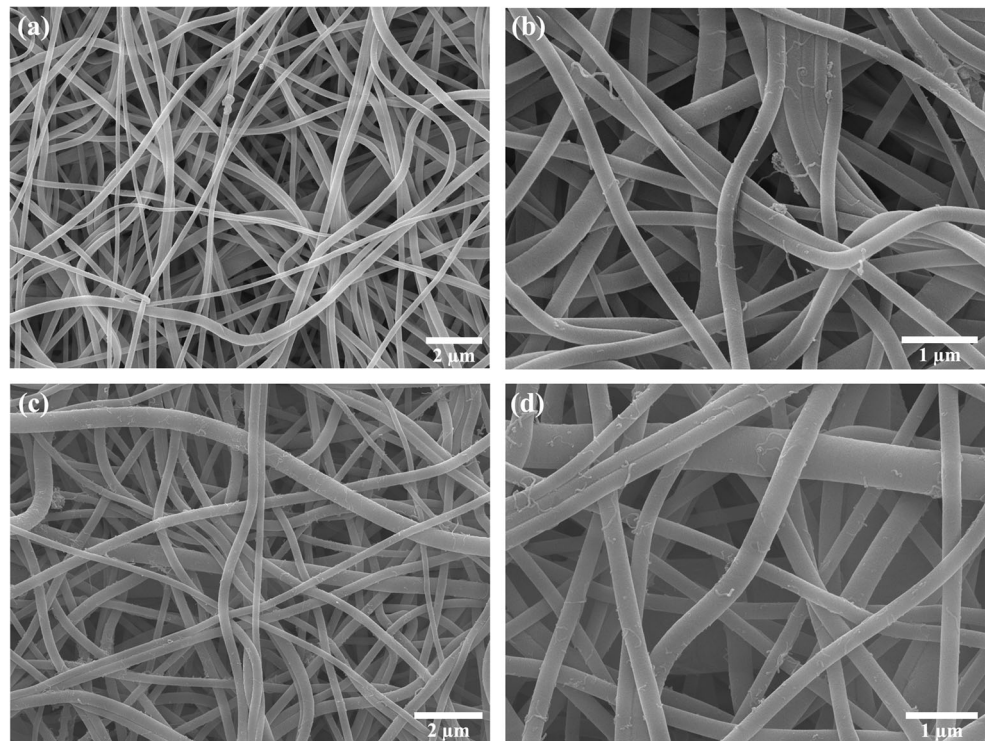
Cd(II), Fe(II), Pb(II), Hg(II), and Ag(I) ions at their MCLs (maximum contaminant levels in drinking water enforced by the U.S. EPA) were employed to investigate their interferences on the response of the Cu(II) sensor to Cu(II) ions. More specifically, 1.3 ppm Cu(II) aqueous solutions containing 0.005 ppm Cd(II), 0.3 ppm Fe(II), 0.015 ppm Pb(II), 0.002 ppm Hg(II), and 0.1 ppm Ag(I), respectively, were prepared. A constant voltage of 1 V was applied to the Cu(II) sensors, and 30 μL of the prepared above solutions was dropped after 30 s. The currents were compared with those corresponding to 1.3 ppm pure Cu(II) aqueous solutions. The MWCNTs/nylon-6 nanocomposites were used for controlled experiments, and the procedures to investigate their resistance and response to Cu(II) ions were the same.

Material characterization The prepared nylon-6 nanofibers, MWCNTs/nylon-6 nanocomposites, and Cu(II) sensors (2,2':5',2''-terthiophene/MWCNTs/nylon-6 nanocomposites) were imaged by a JEOL 6500F scanning electron microscope (SEM). A thin layer of gold was sputter coated on their surfaces and the accelerating voltage was 15 kV. Fourier-transform infrared spectroscopy (FT-IR) was performed on a Bruker ALPHA FT-IR spectrometer. A resolution of 2 cm^{-1} in the range of $4000\text{--}500\text{ cm}^{-1}$ with 30 scans was applied. Thermogravimetric analysis (TGA) curves were acquired at a heating rate of $10\text{ }^\circ\text{C}/\text{min}$ from room temperature to $600\text{ }^\circ\text{C}$ under a N_2 atmosphere through a TA Instruments Q500 thermogravimetric analyzer.

3 Results and discussion

The SEM images of the prepared nylon-6 nanofibers, MWCNTs/nylon-6 nanocomposites, and Cu(II) sensors are exhibited in Fig. 2. The nylon-6 nanofiber has a uniform diameter of about 250 nm and smooth surface, as shown in Fig. 2a. This demonstrates the electrospinning process is steady and consistent. The electrospun nylon-6 mat with non-woven fibrous morphology is free of defects and can perform as an ideal supportive scaffold. It can be seen from Fig. 2b that the MWCNTs are successfully loaded and well dispersed onto the surface of nylon-6 nanofibers. There is no obvious difference between the Fig. 2b, and c and d, which means that the MWCNTs are still firmly anchored to the surface of nylon-6 nanofibers after the introduction of 2,2':5',2''-terthiophene through dip-coating process. The copper binding agent

Fig. 2 SEM images of **a** nylon-6 nanofibers, **b** MWCNTs/nylon-6 nanocomposites, and **c, d** Cu(II) sensors

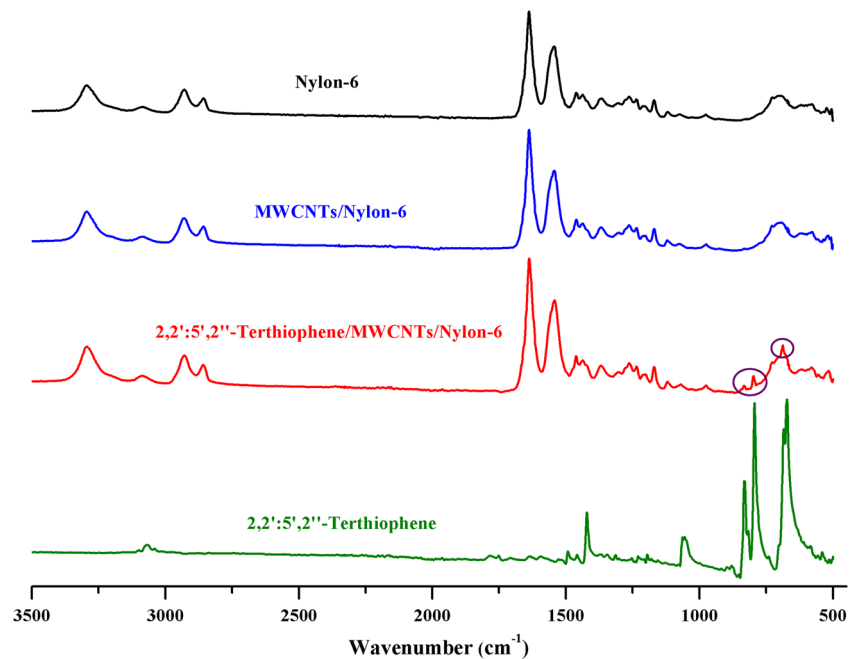


2,2':5',2''-terthiophene molecules are in molecular level thus cannot be observed in SEM images.

Figure 3 shows the FT-IR spectra of nylon-6 nanofibers, MWCNTs/nylon-6 nanocomposites, Cu(II) sensors, and 2,2':5',2''-terthiophene, respectively. The nylon-6 nanofibers and MWCNTs/nylon-6 nanocomposites exhibit the same spectra, which suggests the MWCNTs are bonded onto the surface of nylon-6 electrospun fiber through physical

interactions (Van der Waals force) rather than covalent or ionic bonds. (The overlapped spectra are shown in Fig. S1, as well as the peak positions given in Table S1. The differences on two spectra are negligible as the IR absorbances are well matched and the peak shifts are within 2 cm^{-1} .) Compared with the samples without functional molecules, there are three additional peaks within a range of 875 to 625 cm^{-1} for the Cu(II) sensors. These are attributed to the carbon-hydrogen

Fig. 3 FT-IR spectra of nylon-6 nanofibers, MWCNTs/nylon-6 nanocomposites, Cu(II) sensors, and 2,2':5',2''-terthiophene molecules



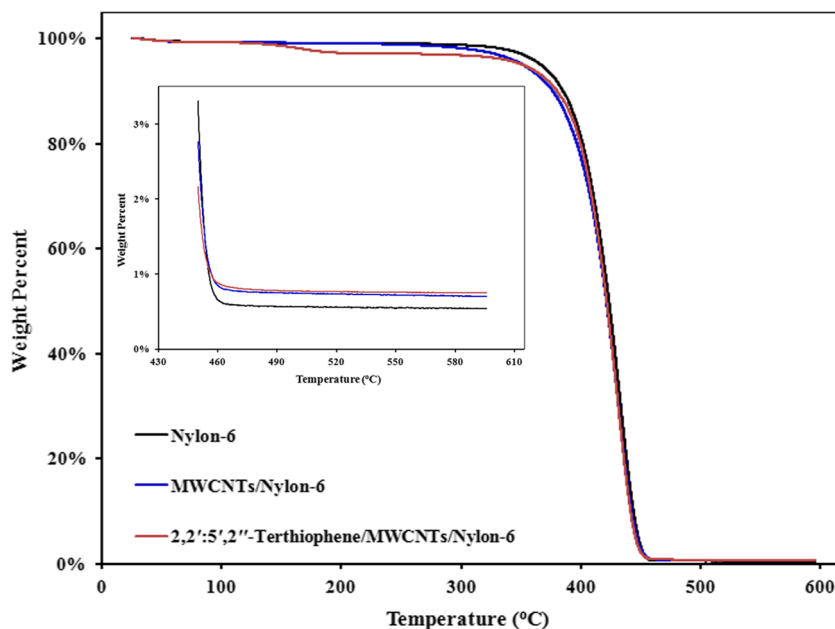
out-of-plane vibrations in thiophene rings, which are also observed in the FT-IR spectrum of 2,2':5',2''-terthiophene. Thus, the 2,2':5',2''-terthiophene molecules are successfully loaded onto the MWCNTs/nylon-6 nanocomposites. By further coupling with the previous SEM images, the successful fabrication of Cu(II) sensors containing MWCNTs and 2,2':5',2''-terthiophene are confirmed.

TGA is employed to investigate the amount of MWCNTs and 2,2':5',2''-terthiophene molecules adsorbed onto the nylon-6 nanofibers, and their TGA curves under nitrogen atmosphere are exhibited in Fig. 4. It shows that the pure electrospun nylon-6 nanofibers are thermally stable until 330 °C. Subsequently, from 330 through 460 °C is the degradation stage of the polymer, leaving the carbonaceous residue about 0.7 wt%. The observed thermogram of pure nylon-6 under nitrogen atmosphere in present study is consistent with the literature [37]. Since MWCNTs are kept intact after the pyrolysis process (as the MWCNTs are thermally stable up to ~1300 °C under the inert environment) [38], the MWCNTs/nylon-6 nanocomposites and Cu(II) sensors have a slightly greater weight percent on residue (see TGA curves of inset in Fig. 4). The difference on residue weight percentages is about 0.2 wt% which is ascribed to the intact MWCNTs. Compared with nylon-6 nanofibers, a lower onset temperature of the degradation is observed for MWCNTs/nylon-6 nanocomposites and Cu(II) sensors (280 °C as opposed to 330 °C for pure nylon-6), which can be partially attributed to the high thermal conductivity of MWCNTs (2×10^2 W/m K) [39]. The faster and easier local heat transfer readily degrades the nylon-6 through the breakages of amide bond in nylon-6 backbone chains leading to a lower onset decomposition temperature [40]. Other than the thermal conductivity, a trace amount of

water in the MWCNTs will also aid the hydrolysis and degradation of the nylon-6 [41]. The defects and acid groups such as $-\text{COOH}$ on the MWCNTs caused by the acid treatment during the synthesis process as well as the residual surfactant Triton X-100 might also impair the thermal stability of nylon-6 which induces the degradation. There is a small weight loss observed at 180 °C for the TGA curve of Cu(II) sensors, which is relating to the evaporation of the 2,2':5',2''-terthiophene molecules. The 2,2':5',2''-terthiophene has a boiling point of 160 °C, and it increases to some extent as a result of the interactions with the nylon-6 and MWCNTs. These TGA results further confirm that the MWCNTs and 2,2':5',2''-terthiophene are successfully loaded onto the nylon-6 nanofibers scaffold and the relative weight percentages are determined to be 0.2 wt% and 2 wt%, respectively.

Figure 5a shows the current-voltage characteristics of the MWCNTs/nylon-6 nanocomposites and Cu(II) sensors in contact of deionized water. The MWCNTs exhibit typically semiconducting behaviors, as observed from the nonlinear data points of the MWCNTs/nylon-6 nanocomposites, while the Cu(II) sensors had more linear data points and metallic characteristics due to the addition of 2,2':5',2''-terthiophene. In order to easily compare their resistances, an approximately linear relationship between the current and voltage is assumed for both the MWCNTs/nylon-6 nanocomposites ($R^2 = 0.97$) and Cu(II) sensors ($R^2 = 0.99$), which means that their resistances are considered stable and constant within a range of -3 to 3 V as pure resistors. The slope of the current-voltage line for the Cu(II) sensors is greater than that for the MWCNTs/nylon-6 nanocomposites, which clearly indicates that the Cu(II) sensors have a lower resistance and a higher electrical conductivity than the MWCNTs/nylon-6 nanocomposites,

Fig. 4 TGA curves of nylon-6 nanofibers, MWCNTs/nylon-6 nanocomposites, and Cu(II) sensors (heating rate 10 °C/min; atmosphere N_2)



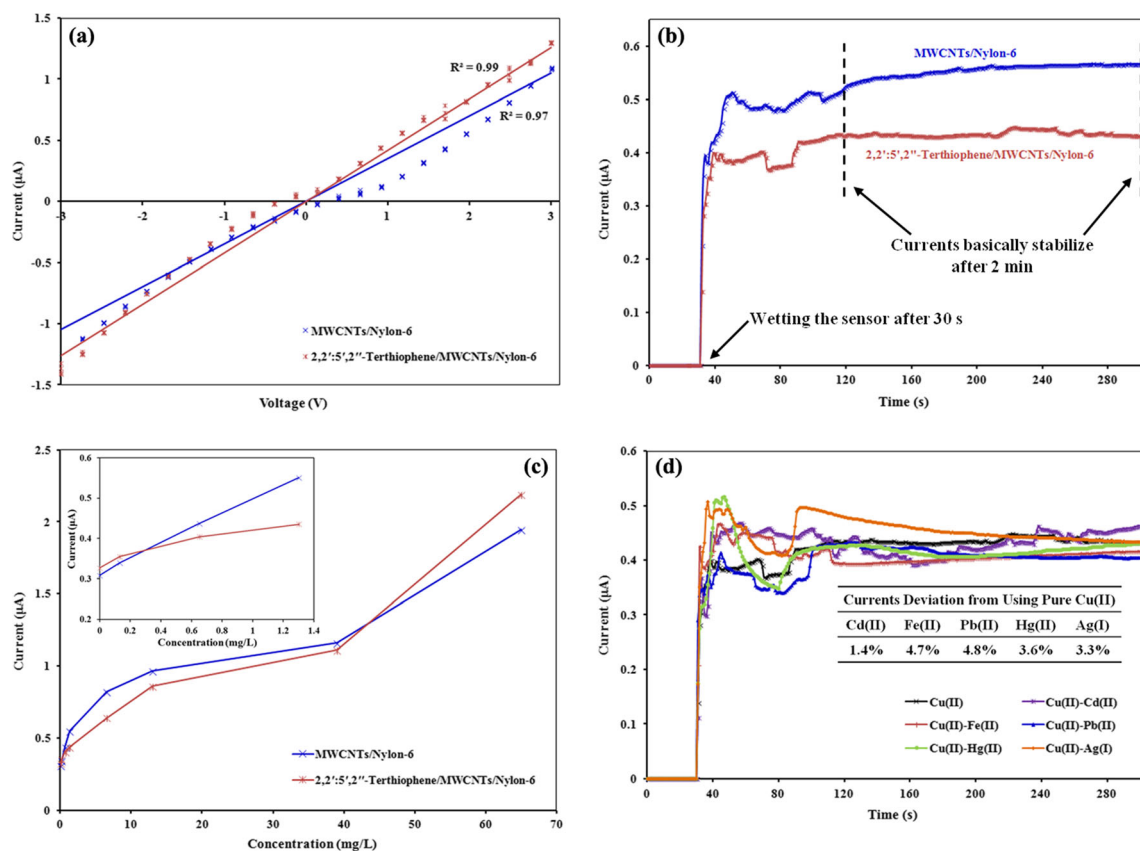


Fig. 5 **a** Current-voltage characteristics of MWCNTs/nylon-6 nanocomposites and Cu(II) sensors wetted by 30 μ L of deionized water (measuring time 2 min). **b** Responses of MWCNTs/nylon-6 nanocomposites and Cu(II) sensors wetted by 30 μ L of Cu(II) aqueous solution at a concentration of 1.3 ppm. **c** Responses of MWCNTs/nylon-6 nanocomposites and Cu(II) sensors wetted by 30 μ L of Cu(II) aqueous solution at different

concentrations. **d** Responses of Cu(II) sensors wetted by 30 μ L of various metal ion aqueous solution (Cu(II) 1.3 ppm; Cu(II)-Cd(II) 1.3–0.005 ppm; Cu(II)-Fe(II) 1.3–0.3 ppm; Cu(II)-Pb(II) 1.3–0.015 ppm; Cu(II)-Hg(II) 1.3–0.002 ppm; Cu(II)-Ag(I) 1.3–0.1 ppm). For Fig. 5b–d, the applied voltage is 1 V.

which can be ascribed to the conductive nature of π stacking molecular structure from the solid state 2,2':5',2''-terthiophene formed on MWCNTs [42–44].

The same amount of 30 μ L Cu(II) aqueous solution at its MCL (1.3 ppm) was dropped onto the MWCNTs/nylon-6 nanocomposites and Cu(II) sensor after 30 s, and the monitored currents gradually became stable after 2 min. The final current is determined by averaging the current readings from 2 to 5 min. As shown in Fig. 5b, the Cu(II) sensor has a significant response to Cu(II) ions. The current in the MWCNTs/nylon-6 nanocomposites is about 1.27 times greater than that of the Cu(II) sensor. Note that the Cu(II) has a higher electrical conductivity in deionized water without Cu(II) ions than the MWCNTs/nylon-6 nanocomposites. In other words, the monitored stable current greatly decreases after replacing the MWCNTs/nylon-6 nanocomposites with Cu(II) sensor. This phenomenon is due to the binding of Cu(II) ions to the 2,2':5',2''-terthiophene molecules on the surface of the Cu(II) sensor which greatly hinders the mobility of carrier charges.

The effects of the Cu(II) concentrations on the responses of the MWCNTs/nylon-6 nanocomposites and Cu(II) sensors

were further investigated. The currents both increase with the increase of Cu(II) concentration due to the ionic nature of Cu(II) ions in aqueous solution, as shown in Fig. 5c. Moreover, there are two intersections between the current-concentration curves of the Cu(II) sensor and MWCNTs/nylon-6 nanocomposites. Since very few Cu(II) ions are present at the ultralow Cu(II) concentrations (<0.2 mg/L), the current flow in the Cu(II) sensor is still greater than that in the MWCNTs/nylon-6 nanocomposites attributed to the lower inherent resistance of the Cu(II) sensor. More Cu(II) ions forming complexes with 2,2':5',2''-terthiophene molecules as the Cu(II) concentration increases, and the current impedance caused by those complexes gradually becomes the main influencer. As a result, the current in the Cu(II) sensor gets smaller than that of the MWCNTs/nylon-6 nanocomposites. However, at high Cu(II) concentrations (>40 mg/L), the slopes of the current-concentration curves for the Cu(II) sensor becomes higher than the MWCNTs/nylon-6 nanocomposites again. This is because the maximum adsorption capacity for Cu(II) ions of the Cu(II) sensor has been reached; thereafter the current is predominantly originated not from the

movement of electrons in MWCNTs but from the conductivity of Cu(II) aqueous solution. Compared with the MWCNTs/nylon-6 nanocomposites, the Cu(II) sensor has strong hydrophobicity with the account of the hydrophobic 2,2':5',2''-terthiophene molecules. Therefore, less Cu(II) aqueous solution is stuck in the Cu(II) sensor, and the current is larger than that of the MWCNTs/nylon-6 nanocomposites. Based on the above analysis, the Cu(II) sensor exhibits an obvious response to Cu(II) ions at Cu(II) concentrations between those two intersections that are considered to be the working range of the Cu(II) sensor, namely from 0.65 to 39 ppm. The 0.65 ppm is 50% lower than the MCL of 1.3 ppm enforced by the U.S. EPA for Cu(II) ions in drinking water, which means that the Cu(II) sensor in our work is suitable and sensitive enough for detecting Cu(II) ions in drinking water. Meanwhile, the upper limit of 39 ppm is ~30 times of the EPA MCL demonstrating the sensor is applicable for a wide range of the Cu(II) contaminated water.

When a voltage is being applied to the Cu(II) sensor, an electric current is generated as electrons flow through the MWCNTs. The Cu(II) ions that are captured by 2,2':5',2''-terthiophene molecules can draw away some electrons from the MWCNTs due to their positive charges; therefore, a responsive change (a decrease) in current will be observed. Since the 2,2':5',2''-terthiophene molecules have a much high selectivity towards Cu(II) ions over the other metal ions, the response of the Cu(II) sensor should remain the same with the existence of interfering metal ions. In other words, there should be no obvious change for the current when other metal ions are introduced into the aqueous solution. In order to be more practical, Cd(II), Fe(II), Pb(II), Hg(II), and Ag(I) at their MCLs set by the U.S. EPA were employed into the Cu(II) aqueous solutions to investigate their interferences on the response of the Cu(II) sensor to Cu(II) ions. It can be seen from Fig. 5d that the currents hardly change (less than 5%) when different interfering metal ion aqueous solutions, instead of pure Cu(II) aqueous solution, are used. Pb(II) and Fe(II) show slightly greater effects with current differences of 4.8% and 4.7%, respectively. Compared with the sensor sensitivity of Cu(II), the interferences of these metal ions are negligible. Thus, the Cu(II) sensor is able to selectively detect Cu(II) ions among various other interfering metal ions in water.

4 Conclusion

Detection of Cu(II) ions in drinking water is usually a bigger challenge than in other contaminated water as a result of its much lower MCLs. A sensitive, cost-effective, flexible, and portable amperometric sensor is successfully prepared via a simple dip-coating method in this work, which is composed of electrospun nylon-6 nanofibers, MWCNTs, and 2,2':5',2''-terthiophene molecules. Owing to the selective binding of

2,2':5',2''-terthiophene molecules with Cu(II) ions, the fabricated sensor shows a significant response to Cu(II) ions in a wide range of 0.65 to 39 ppm, which indicates that its detection limit is way lower than the MCL (1.3 ppm) for Cu(II) ions. Moreover, the Cu(II) sensor exhibits a superior selectivity towards Cu(II) ions over other metal ions, and the presence of Cd(II), Fe(II), Pb(II), Hg(II), and Ag(I) ions at their MCLs has no obvious interfering effects on its response to Cu(II) ions. Therefore, the Cu(II) sensor in this work shows promise in monitoring Cu(II) ions in drinking water in real time.

Acknowledgments This work was supported by The University of Alabama College of Engineering.

Funding information This work was financially supported by the Texas Hazardous Waste Research Center [THWRC].

Compliance with ethical standards

Conflict of interest The authors declare that they have no conflict of interest.

References

1. C. f. D. C. a. Prevention. Copper and drinking water from private wells. [cdc.gov. https://www.cdc.gov/healthywater/drinking/private/wells/disease/copper.html](https://www.cdc.gov/healthywater/drinking/private/wells/disease/copper.html). Accessed 2017
2. Mukherjee S, Talukder S, Chowdhury S, Mal P, Stoeckli-Evans H (2016) Synthesis, structure and sensing behavior of hydrazone based chromogenic chemosensors for Cu²⁺ in aqueous environment. *Inorg Chim Acta* 450:216–224. <https://doi.org/10.1016/j.ica.2016.05.049>
3. Lv L, Diao Q (May 15 2017) A highly selective and sensitive rhodamine-derived fluorescent probe for detection of Cu²⁺. *Spectrochim Acta A Mol Biomol Spectrosc* 179:221–226. <https://doi.org/10.1016/j.saa.2017.02.053>
4. Wang S et al (2017) The triple roles of glutathione for a DNA-cleaving DNAzyme and development of a fluorescent glutathione/Cu²⁺-dependent DNAzyme sensor for detection of Cu²⁺ in drinking water. *ACS Sens* 2(3):364–370. <https://doi.org/10.1021/acssensors.6b00667>
5. Zong L, Song Y, Li Q, Li Z (2016) A “turn-on” fluorescence probe towards copper ions based on core-substituted naphthalene diimide. *Sensors Actuators B Chem* 226:239–244. <https://doi.org/10.1016/j.snb.2015.11.089>
6. He Y et al (2016) Phosphatidylserine-functionalized Fe₃O₄@SiO₂ nanoparticles combined with enzyme-encapsulated liposomes for the visual detection of Cu²⁺. *J Mater Chem B* 4(4):752–759. <https://doi.org/10.1039/c5tb01926e>
7. Gedda G, Lee C-Y, Lin Y-C, Wu H-F (2016) Green synthesis of carbon dots from prawn shells for highly selective and sensitive detection of copper ions. *Sensors Actuators B Chem* 224:396–403. <https://doi.org/10.1016/j.snb.2015.09.065>
8. Su Y et al (2016) Facile preparation of fluorescent polydihydroxyphenylalanine nanoparticles for label-free detection of copper ions. *Sensors Actuators B Chem* 225:334–339. <https://doi.org/10.1016/j.snb.2015.11.067>
9. Xiong J-J, Huang P-C, Zhou X, Wu F-Y (2016) A highly selective and sensitive “turn-on” fluorescent probe of Cu²⁺ by p-dimethylaminobenzamide-based derivative and its bioimaging in

- living cells. *Sensors Actuators B Chem* 232:673–679. <https://doi.org/10.1016/j.snb.2016.04.004>
10. Gao W et al (2016) Wearable microsensor array for multiplexed heavy metal monitoring of body fluids. *ACS Sens* 1(7):866–874. <https://doi.org/10.1021/acssensors.6b00287>
 11. Huang J, Zheng Q, Kim JK, Li Z (2013) A molecular beacon and graphene oxide-based fluorescent biosensor for Cu²⁺ detection. *Biosens Bioelectron* 43:379–383. <https://doi.org/10.1016/j.bios.2012.12.056>
 12. Pihlasalo S, Perez IM, Hollo N, Hokkanen E, Pahikkala T, Harma H (2016) Luminometric label array for quantification and identification of metal ions. *Anal Chem* 88(10):5271–5280. <https://doi.org/10.1021/acs.analchem.6b00453>
 13. Kang JH, Lee SY, Ahn HM, Kim C (2016) Sequential detection of copper(II) and cyanide by a simple colorimetric chemosensor. *Inorg Chem Commun* 17:62–65. <https://doi.org/10.1016/j.inoche.2016.10.039>
 14. Rezaeian K, Khanmohammadi H, Arab V (Dec 05 2015) Rational design of a novel azoimine appended maleonitrile-based Salen chemosensor for rapid naked-eye detection of copper(II) ion in aqueous media. *Spectrochim Acta A Mol Biomol Spectrosc* 151: 848–853. <https://doi.org/10.1016/j.saa.2015.06.127>
 15. Zhang H et al (2015) Coupling a novel spiro-rhodamine B lactam derivative to Fe₃O₄ nanoparticles for visual detection of free copper ions with high sensitivity and specificity. *RSC Adv* 5(57): 45847–45852. <https://doi.org/10.1039/c5ra04272k>
 16. Wujcik EK, Duirk SE, Chase GG, Monty CN (2016) A visible colorimetric sensor based on nanoporous polypropylene fiber membranes for the determination of trihalomethanes in treated drinking water. *Sensors Actuators B Chem* 223:1–8. <https://doi.org/10.1016/j.snb.2015.09.004>
 17. Zhang B, Diao Q, Ma P, Liu X, Song D, Wang X (2016) A sensitive fluorescent probe for Cu²⁺ based on rhodamine B derivatives and its application to drinking water examination and living cells imaging. *Sensors Actuators B Chem* 225:579–585. <https://doi.org/10.1016/j.snb.2015.11.069>
 18. Huang P-C, Fang H, Xiong J-J, Wu F-Y (2017) Ultrasensitive turn-on fluorescence detection of Cu²⁺ based on p-dimethylaminobenzamide derivative and the application to cell imaging. *Spectrochim Acta A Mol Biomol Spectrosc* 173:264–269. <https://doi.org/10.1016/j.saa.2016.09.011>
 19. Shanmugaraj K, Ilanchelian M (2016) A “turn-off” fluorescent sensor for the selective and sensitive detection of copper(II) ions using lysozyme stabilized gold nanoclusters. *RSC Adv* 6(59):54518–54524. <https://doi.org/10.1039/c6ra08325k>
 20. Khan B et al (2016) Synthesis, characterization and Cu²⁺ triggered selective fluorescence quenching of bis-calix[4]arene tetra-triazole macrocycle. *J Hazard Mater* 309:97–106. <https://doi.org/10.1016/j.jhazmat.2016.01.074>
 21. Vopalenska I, Vachova L, Palkova Z (2015) New biosensor for detection of copper ions in water based on immobilized genetically modified yeast cells. *Biosens Bioelectron* 72:160–167. <https://doi.org/10.1016/j.bios.2015.05.006>
 22. Wang R, Wang W, Ren H, Chae J (2014) Detection of copper ions in drinking water using the competitive adsorption of proteins. *Biosens Bioelectron* 57:179–185. <https://doi.org/10.1016/j.bios.2014.01.056>
 23. Yin K, Wu Y, Wang S, Chen L (2016) A sensitive fluorescent biosensor for the detection of copper ion inspired by biological recognition element pyoverdine. *Sensors Actuators B Chem* 232: 257–263. <https://doi.org/10.1016/j.snb.2016.03.128>
 24. Zhang W et al (2012) Self-assembled multilayer of alkyl graphene oxide for highly selective detection of copper(II) based on anodic stripping voltammetry. *J Mater Chem* 22(42):22631–22636. <https://doi.org/10.1039/c2jm34795d>
 25. Sun Y-F, Zhao L-J, Jiang T-J, Li S-S, Yang M, Huang X-J (2016) Sensitive and selective electrochemical detection of heavy metal ions using amino-functionalized carbon microspheres. *J Electroanal Chem* 760:143–150. <https://doi.org/10.1016/j.jelechem.2015.11.028>
 26. Li W-J, Yao X-Z, Guo Z, Liu J-H, Huang X-J (2015) Fe₃O₄ with novel nanoplate-stacked structure: surfactant-free hydrothermal synthesis and application in detection of heavy metal ions. *J Electroanal Chem* 749:75–82. <https://doi.org/10.1016/j.jelechem.2015.04.038>
 27. Yuan S, Peng D, Hu X, Gong J (2013) Bifunctional sensor of pentachlorophenol and copper ions based on nanostructured hybrid films of humic acid and exfoliated layered double hydroxide via a facile layer-by-layer assembly. *Anal Chim Acta* 785:34–42. <https://doi.org/10.1016/j.aca.2013.04.050>
 28. Xiong S, Ye S, Hu X, Xie F (2016) Electrochemical detection of ultra-trace Cu(II) and interaction mechanism analysis between amine-groups functionalized CoFe₂O₄/reduced graphene oxide composites and metal ion. *Electrochim Acta* 217:24–33. <https://doi.org/10.1016/j.electacta.2016.09.060>
 29. Wang S, Wang Y, Zhou L, Li J, Wang S, Liu H (2014) Fabrication of an effective electrochemical platform based on graphene and AuNPs for high sensitive detection of trace Cu²⁺. *Electrochim Acta* 132:7–14. <https://doi.org/10.1016/j.electacta.2014.03.114>
 30. Soleimani M, Afshar MG (2013) Potentiometric sensor for trace level analysis of copper based on carbon paste electrode modified with multi-walled carbon nanotubes. *Int J Electrochem Sci* 8:8719–8729
 31. Baig U, Khan AA (2015) Polyurethane-based cation exchange composite membranes: preparation, characterization and its application in development of ion-selective electrode for detection of copper(II). *J Ind Eng Chem* 29:392–399. <https://doi.org/10.1016/j.jiec.2014.12.045>
 32. Ali TA, Eldidamony AM, Mohamed GG, Elatfy DM (2014) Construction of chemically modified electrode for the selective determination of copper(II) ions in polluted water samples based on new β-cyclodextrine and 1,4-bis(6-bromo-hexyloxy)benzene ionophores. *Int J Electrochem Sci* 9:2420–2434
 33. Mahajan RK, Sood P (2007) Novel copper(II)-selective electrode based on 2,2':5,2"-terthiophene in PVC matrix. *Int J Electrochem Sci* 2:832–847
 34. Wujcik EK, Blasdel NJ, Trowbridge D, Monty CN (2013) Ion sensor for the quantification of sodium in sweat samples. *IEEE Sensors J* 13(9):3430–3436. <https://doi.org/10.1109/jsen.2013.2257168>
 35. Lala NL, Thavasi V, Ramakrishna S (2009) Preparation of surface adsorbed and impregnated multi-walled carbon nanotube/nylon-6 nanofiber composites and investigation of their gas sensing ability. *Sensors* 9(1):86–101. <https://doi.org/10.3390/s90100086>
 36. Monty CN, Wujcik EK, Blasdel NJ (2017) Flexible electrode for detecting changes in temperature, humidity, and sodium ion concentration in sweat. USA Patent US 9,603,560 B2 Patent Appl. 61/590,839
 37. El-Newehy MH, Al-Deyab SS, Kenawy E-R, Abdel-Megeed A (2011) Nanospider technology for the production of nylon-6 nanofibers for biomedical applications. *J Nanomater* 2011:1–8. <https://doi.org/10.1155/2011/626589>
 38. Mahajan A, Kingon A, Kukovec A, Konya Z, Vilarinho PM (2013) Studies on the thermal decomposition of multiwall carbon nanotubes under different atmospheres. *Mater Lett* 90:165–168
 39. Zhang Q et al (2002) Thermal conductivity of multiwalled carbon nanotubes. *Phys Rev B* 66(16):165440
 40. Chen G-X, Kim H-S, Park BH, Yoon J-S (2006) Multi-walled carbon nanotubes reinforced nylon 6 composites. *Polymer* 47(13): 4760–4767

41. Choi J, Park DW, Shim SE (2011) Chemical vapour sensing behaviors of multi-walled carbon nanotube adsorbed electrospun nylon 6, 6 nanofibers. *Macromol Res* 19(9):980–983. <https://doi.org/10.1007/s13233-011-0905-x>
42. Yin B, Jiang C, Wang Y, La M, Liu P, Deng W (2010) Synthesis and electrochromic properties of oligothiophene derivatives. *Synth Met* 160(5–6):432–435. <https://doi.org/10.1016/j.synthmet.2009.11.025>
43. Generali G, Capelli R, Toffanin S, Facchetti A, Muccini M (2010) Ambipolar field-effect transistor based on α,ω -dihexylquaterthiophene and α,ω -diperfluoroquaterthiophene vertical heterojunction. *Microelectron Reliab* 50(9–11):1861–1865. <https://doi.org/10.1016/j.microrel.2010.07.047>
44. Pappenfus TM et al (2002) A π -stacking terthiophene-based quinodimethane is an n-channel conductor in a thin film transistor. *J Am Chem Soc* 124(16):4184–4185

Publisher's note Springer Nature remains neutral with regard to jurisdictional claims in published maps and institutional affiliations.